J Mater Sci (2016) 51:5685–5694

A green method for preparation of CNT/CS/AgNP composites and evaluation of their catalytic performance

Yanpeng Dou[1], Honglin Liu[1], Junjun Peng[1,*], Ming Li[1], Wei Li[1], and Feng Yang[1]

[1] College of Chemistry and Chemical Engineering, Wuhan Textile University, Wuhan 430200, People's Republic of China

Received: 13 July 2015
Accepted: 1 March 2016
Published online: 8 March 2016

ABSTRACT

In this work, a green method was employed to prepare CNT/CS/AgNP composites, and the catalytic performance of the composites was evaluated. Firstly, carbon nanotubes were modified by chitosan molecules to generate carbon nanotube/chitosan (CNT/CS) composites. Then, silver ions were absorbed and in situ reduced to Ag nanoparticles by the CNT/CS composites, forming CNT/CS/AgNP composites without any other reductants. UV–Visible spectra, Fourier transform infrared spectroscopy, X-ray diffraction, transmission electron microscopy, and thermogravimetric analysis were employed to analyze the composition, crystalline structure, morphology, and thermal stability of CNT/CS/AgNP composites. The results showed the average size of silver nanoparticles was 6 nm, and the Ag particles were uniformly distributed on the surface of carbon nanotubes. Overall, the CNT/CS/AgNP composites showed high catalytic activity for hydrogenation reduction of *p*-nitrophenol with a rate constant of 0.257 min^{-1} and an activation energy of 89.27 kJ mol^{-1}.

Introduction

CNT/AgNP composites are the mixture of Ag nanoparticles (AgNPs) and carbon nanotubes (CNTs), and are widely applied in electrochemical catalysis [1, 2], in biosensor [3, 4], as antibacterial agents [5, 6], and as conductivity films [7, 8]. The CNT/AgNP composites have been prepared by thermal deposition [9], chemical reduction deposition [10, 11], and electrodeposition [12], etc. However, owing to carbon nanotubes' hydrophobic nature and insolubility in most solvents, it is difficult for silver nanoparticles to be uniformly dispersed on the surface of carbon nanotubes. Therefore, different routes were designed to modify the surface properties of carbon nanotubes [13–16] and make sufficient biding sites for anchoring metal nanoparticles [17]. In order to improve the dispersion of carbon nanotubes in solutions, strong-acid-oxidation method has been commonly used to generate carboxyl and hydroxyl groups on the carbon nanotubes' surface, which is advantageous to adhere with nanometer-sized materials [18–20]. However, this method can result in carbon nanotubes' fragmentation and defect

Address correspondence to E-mail: john_peng@whu.edu.cn

DOI 10.1007/s10853-016-9871-1

generation in the graphitic network, as well as generate a large amount of highly corrosive acid waste solution, which may severely pollute the environment. Moreover, it is a time-consuming and cumbersome process.

Chitosan (CS) is a natural biopolymer and has lots of amino and hydroxyl groups, which could be used to decorate the surface of carbon nanotubes and act as a polymer cationic surfactant to stabilize carbon nanotubes. The technological process is very simple and environmentally friendly [21]. In addition, chitosan has been used as a green reductant and stabilizing agent reducing silver ion to silver nanoparticles [22]. Silver nanoparticles/carbon nanotubes/chitosan film was reported to be applied in glucose biosensor [23] and bionanocomposite thin films [24]. However, chitosan was just employed as biocompatible immobilization matrix, and Ag nanoparticles were synthesized using different reductants, such as trisodium citrate and $NaBH_4$ [23, 24].

In this paper, a green method was reported to prepare highly dispersed Ag nanoparticles on the surface of carbon nanotubes. Chitosan was employed to decorate carbon nanotubes, forming CNT/CS composites. Then, the CNT/CS composites in situ absorbed and reduced silver ions to Ag nanoparticles without any extra reductants, generating CNT/CS/AgNP composites. The composition, crystalline structure, morphology, and thermal stability of CNT/CS/AgNP composites were characterized by UV–Visible spectrophotometer, Fourier transform infrared spectroscopy (FTIR), X-ray diffraction (XRD), transmission electron microscopy (TEM), and thermogravimetric analysis (TGA). The catalytic performance of CNT/CS/AgNP composites was evaluated by catalytic hydrogenation reduction of *p*-nitrophenol.

Experiment and methods

Preparation of CNT/CS/AgNP composites

Figure 1 shows the schematic illustration of three-step process for preparing CNT/CS/AgNP composites. Firstly, pristine carbon nanotubes (10–20 nm diameter, <2 μm length, >97 % purity, Shenzhen Nanotech Port Co.) modified with chitosan (degree of deacetylation ≥90 %, Shanghai Ruji Biotech. Co., Ltd.) were prepared as follows: 0.1 g CNT was dispersed in 100 mL chitosan solution (0.1 g chitosan dissolved in 100 mL 1 % acetic acid solutions) under ultrasonic treatment (Kunshan Ultrasonic Instrument Co. Ltd., KQ5200V, 40 kHz) in water bath for 2 h. In this process, chitosan macromolecules were made to adsorb on to the surface of CNTs, which acted as polymer cationic surfactants to stabilize CNTs. Then, ammonia water (25 % w/w) was added dropwise to the solution to coagulate CNT/CS composites, and the black sediment was filtered using sintered glass funnel and washed with ultrapure water until the filtrate was neutral. Lastly, CNT/CS composites were dried by vacuum freezing at −50° for 12 h. All chemicals not mentioned above are of analytical pure and provided by Sinopharm Chemical Reagent Co. Ltd. Ultrapure water (>18.25 MΩ cm) was prepared by UP water purification system (Wuhan ultrapure water purification equipment Co., Ltd.). All chemicals were used as received without any treatment.

In a typical experiment, 50 mg CNT/CS composites were dispersed into 100 mL ultrapure water in a beaker with ultrasonic treatment in a water bath for 1 h, and to this solution, 4.0 mL of $AgNO_3$ (0.125 mol/L) solution was added under magnetic stirring for 30 min at 94 °C, for the absorption of silver ion to occur. Then NaOH solution (5 % w/w)

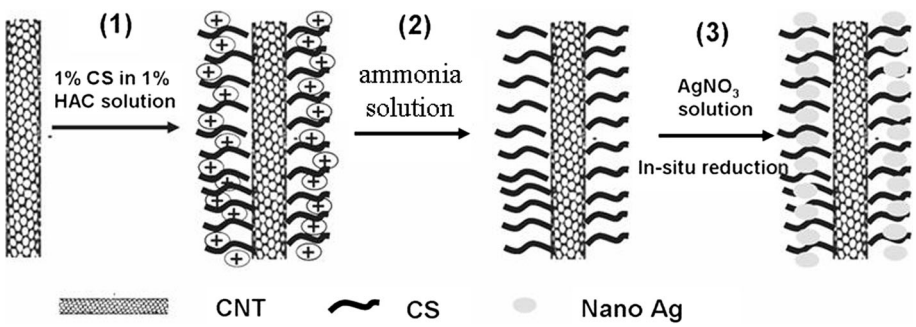

Figure 1 Schematic illustration of preparing CNT/CS/AgNP composites.

was added to adjust the pH value of the solution to 8–9, and thus silver ions can be reduced to silver nanoparticles in this step. The temperature of the solution was also controlled at 94 °C with a hotplate equipment with a magnetic stirrer for 1 h. After that, the reaction solution was filtered using conical funnel and rapid qualitative filter paper at atmospheric pressure, and dried in vacuum oven at 60 °C for 10 h. Thus, the CNT/CS/AgNP composites were obtained. For comparison, CS/AgNP composites were produced by the same process as described above, and 50 mg CS instead of CNT/CS was used to absorb and reduce Ag ions to Ag nanoparticles.

Characterization

The obtained samples in this study were characterized by an X-ray diffraction (SHIMADZU Lab XRD-6000 with Cu Kα1), Fourier transform infrared spectroscopy (FTIR, TENSOR 27, Bruker Corporation), thermogravimetric analysis (TGA, METTLER TOLEDO), and transmission electron microscopy (JEM-2100, JEOL Ltd.). UV–Vis Spectra were measured with a UV–Visible spectrophotometer (TU-1901, Beijing Purkinje General Instrument Co. Ltd.).

Catalytic reduction of 4-nitrophenol

Investigations of the catalytic activity of the prepared CNT/CS/AgNP nanocomposites were done using the reduction of 4-nitrophenol (4-NP) to 4-aminophenol (4-AP) by $NaBH_4$ as a model reaction. Aqueous 4-NP solution (50 mL, 0.266 mM) was mixed with fresh $NaBH_4$ (13.3 mM). The prepared CNT/CS/AgNPs were dispersed in the mixture. To study the effect of temperature on their catalytic performance, the reaction was conducted at five temperatures, i.e., 298.15, 300.15, 303.15, 306.15, and 308.15 K, respectively, in a temperature-controlled water bath. UV–Vis absorption spectra were recorded to determine the variation of the maximum absorption intensity in the wavelength range of 250–500 nm.

Results and discussion

Analysis of CNT/CS/AgNP nanocomposites

Figure 2 shows the UV–Vis absorption spectra of CS, CNT/CS, CS/AgNPs, and CNT/CS/AgNPs dissolved in 1 % HAC solution. It was found that only CS/AgNPs and CNT/CS/AgNPs had an absorption peak at 400 nm, which arose from surface plasmon resonance absorption of silver nanoparticles [25, 26], indicating that chitosan was able to reduce silver ions to silver nanoparticles [22, 27].

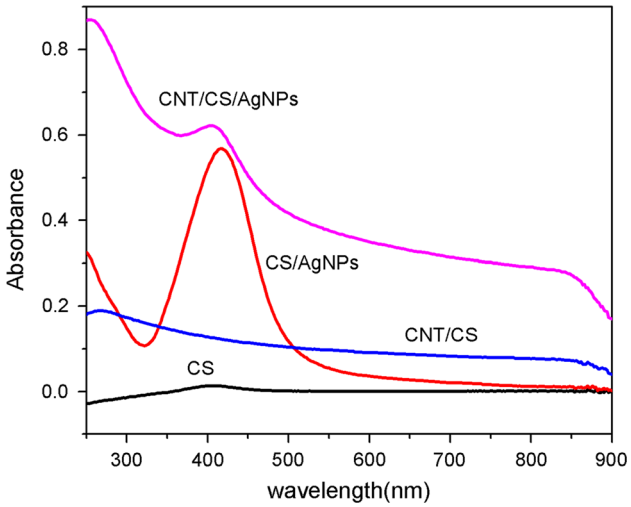

Figure 2 UV–Vis absorption spectrum of different samples as indicated.

FTIR is one of the most important characterization techniques to elucidate the changes of chemical structures. As shown in Fig. 3, broad peaks of CS, CNT, CNT/CS, and CNT/CS/AgNPs appeared at 3439 cm^{-1} due to the stretching vibration of –OH or –NH. Chitosan possessed main peaks at 2848–2920 cm^{-1} due to the bending vibrations of $-CH_2$

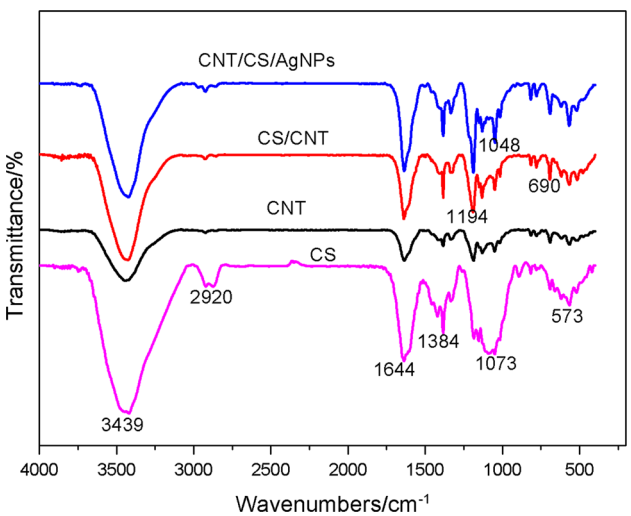

Figure 3 FTIR spectra of CNT/CS/AgNPs, CS/CNT, CNT, and CS samples as indicated.

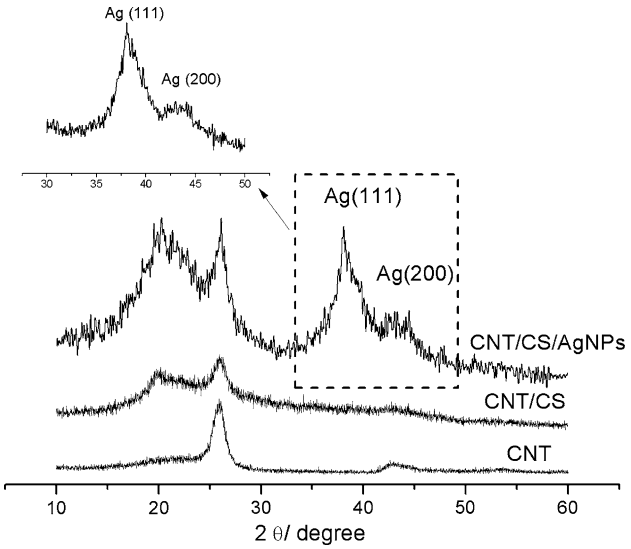

Figure 4 XRD spectra of CNT, CNT/CS, and CNT/CS/AgNP composite samples (the inset is the high-accuracy measurement of CNT/CS/AgNPs with 1 °/min scan rate from 30° to 50°).

groups, and at around 1073 cm^{-1} due to the stretching vibration of C–O–C groups. It was found that the FTIR spectra of CNT/CS and CNT/CS/AgNPs were almost the same, indicating that the formation of Ag nanoparticles could not affect the wave numbers of the chemical bonds of CNT/CS and there was no chemical interaction between Ag nanoparticles and CNT/CS. However, the intensity of peaks at 1644 cm^{-1} (–C=O stretching vibration) and 1194 cm^{-1} (C–O–C stretching vibration) of CNT/CS/AgNPs was much higher than those of CNT/CS, signifying that the attached CS acted as reductant to reduce Ag ions and, simultaneously, the reducible groups of CS, like hydroxyl, were converted into –C=O or C–O–C groups [28].

Figure 4 shows the XRD patterns of pristine CNT, CNT/CS, and CNT/CS/AgNP composites. It can be observed from the figure that there were two broad diffraction peaks of CNT/CS samples with 2θ values of 20.0° and 26.1°, and one peak at 26.1° for pristine CNTs. For CNT/CS/AgNP samples, the diffraction peaks with 2θ values of 20.0° and 26.1° showed the existence of CS and CNT. Moreover, other peaks with 2θ values of 38.17° and 44.21° arose from silver nanoparticles, corresponding to the silver crystallographic plane of 111 and 200. The crystalline grain size of Ag nanoparticles was measured by high-accuracy XRD test with 1°/min scan rate from 30° to 50° (2θ), as shown in the inset of Fig. 4. The size of the crystalline grain is calculated from the major diffraction peak (111) using Scherrer's formula [29]. The average size of crystalline grain of Ag nanoparticles on the surface of carbon nanotubes was about 5.4 nm.

Figure 5 shows the TEM images of CNT/CS/AgNPs and CS/AgNPs. It was found that a large number of small nanoparticles uniformly dispersed and strongly adhered on the surface of carbon

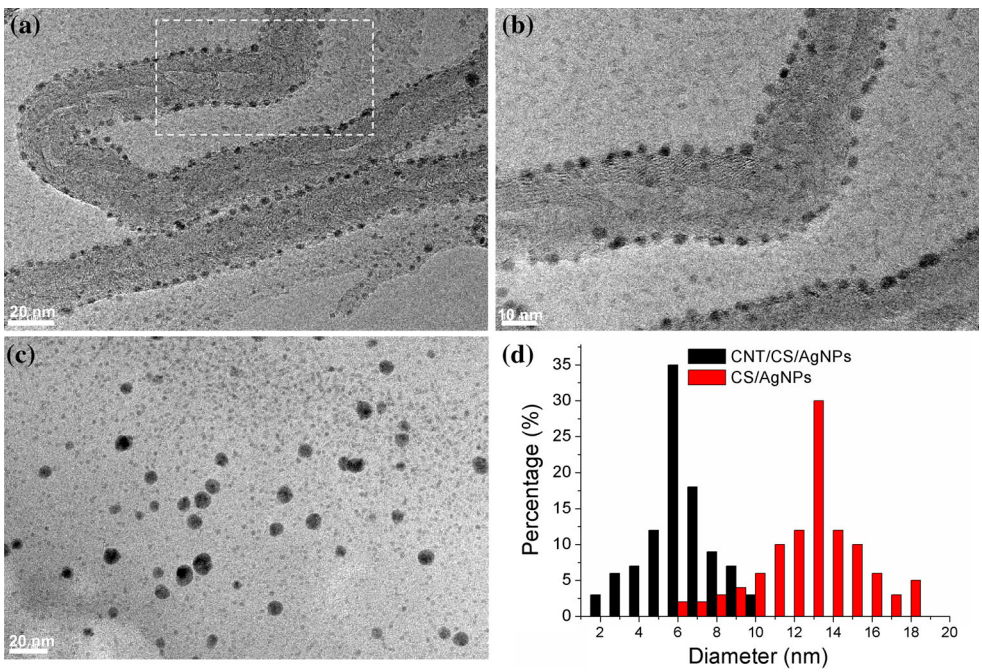

Figure 5 TEM images of samples: **a** CNT/CS/AgNPs, **b** the magnified image of box shown in (**a**), **c** CS/AgNPs. **d** The particle size distribution histogram of (**a**) and (**c**).

nanotubes (as shown in Fig. 5a), which was different from the morphology of silver nanoparticles/carbon nanotubes/chitosan film [23, 24]. The high-magnified TEM image in Fig. 5b reveals that the small particles may be in the range of 2–10 nm in size. The size distribution histogram showed that the average size of Ag nanoparticles was 6 nm (Fig. 5d), which was very close to the result of XRD analysis. In comparison, CS/AgNP samples were prepared by the same method without any reducing agent. The TEM images of CS/AgNP samples in Fig. 5c show that lots of silver nanoparticles were dispersed in chitosan film. The average size of silver nanoparticles of CS/AgNP was about 13 nm as shown in Fig. 5d. Obviously, the size of Ag nanoparticles from CNT/CS/AgNP composites was smaller than that from CS/AgNPs. This is because that the adhered CS on the surface of carbon nanotubes was capable of absorbing silver ions. Moreover, the hydroxyl group of CS enabled the reduction of silver ions to silver nanoparticles in alkaline solution [30], which resulted in the generation of both CNT/CS/AgNPs and CS/AgNPs. However, owing to the combination of CS and CNT, most silver nanoparticles tended to form on the surface of CNT, which may decrease the growth of silver grain. Therefore, it was favorable to obtain silver nanoparticles in smaller size on the surface of carbon nanotubes. Due to the smaller size of Ag particles and their good adherence to CNTs, the CNT/CS/AgNP composites could be a promising catalyst.

The thermal behavior of the prepared CNT/CS/AgNP composites is studied to evaluate its thermal stability and measure the weight ratio of Ag nanoparticles in the composites. Figure 6 shows that CNT/CS/AgNP and CNT/CS composites had undergone apparent weight loss from 200 to 450 °C in N_2 atmosphere. This was attributed to a complex process for chitosan degradation, including dehydration of the saccharide rings, depolymerization and/or decomposition of the acetylated and deacetylated units [31]. Because pristine CNT had a very good thermostability in nitrogen, there was no weight loss below 1000 °C [32]. However, in oxygen atmosphere, for CNT/CS/AgNP composites, there was a very sharp weight loss, about 80 % below 500 °C, which was due to chitosan degradation and CNT oxidation. Then, the weight loss was only about 3 % from 500 to 1000 °C, suggesting that a small residue decomposed at higher temperature. At 1000 °C, chitosan and CNT should be completely

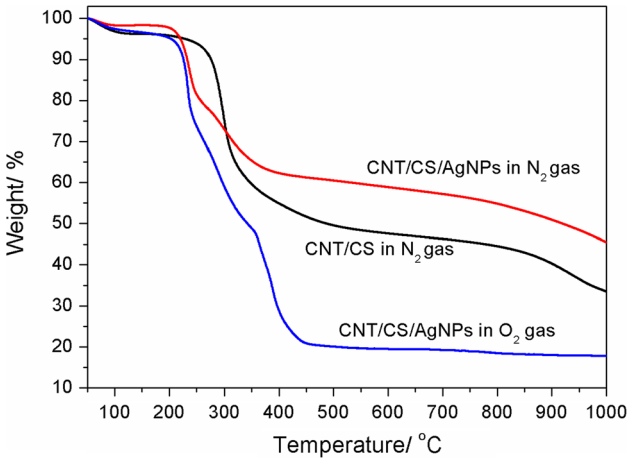

Figure 6 TGA analysis of CNT/CS/AgNP and CNT/CS samples with different atmospheres as indicated.

broken up in oxygen atmosphere [33], but silver was still stable at this temperature. Thus, according to the TG analysis, the weight ratio of silver in CNT/CS/AgNP composites is 18 %.

Catalytic reduction of 4-nitrophenol (4-NP) with CNT/CS/AgNP composites

4-Aminophenol (4-AP) has been widely used as analgesic and antipyretic drug, photographic developer, corrosion inhibitor, anticorrosion lubricant, etc. [34]. 4-AP was usually prepared by the reduction of 4-nitrophenol (4-NP) with $NaBH_4$ in the presence of different catalysts, such as gold, nickel, silver, and other noble metals [35–38]. The catalytic reduction process is represented below.

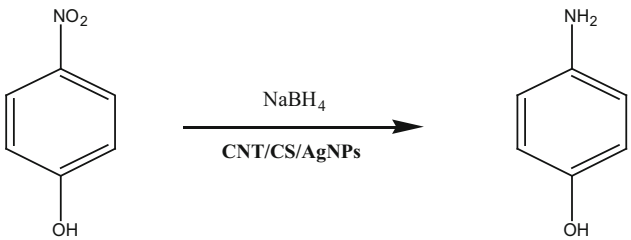

As shown in Fig. 7, aqueous solution of 4-NP shows a distinct spectral profile with an absorption peak being maximum at 317 nm, and the absorption peak shifts to 400 nm in the presence of $NaBH_4$ due to the formation of 4-nitrophenolate ion [39]. Without addition of the CNT/CS/AgNP catalysts, no color change of the aqueous solution was observed at room temperature. The color of the solution changed

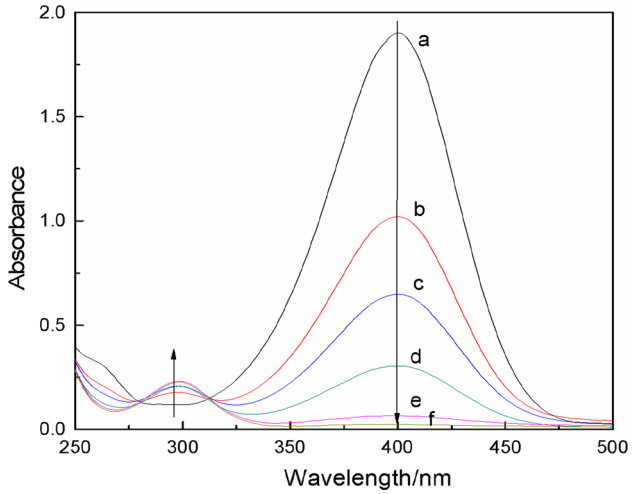

Figure 7 Typical UV–Vis spectra of the gradual reduction of 4-NP by $NaBH_4$ in aqueous solution at 25 °C with CNT/CS/AgNP composites serving as the catalyst. Curves from **a** to **f** are obtained from 0, 4, 8, 12, 16, and 20 min ($m_{CNT/CS/AgNPs} = 2$ mg, [4-NP] = 37 mg/L, [$NaBH_4$] = 1.85 g/L).

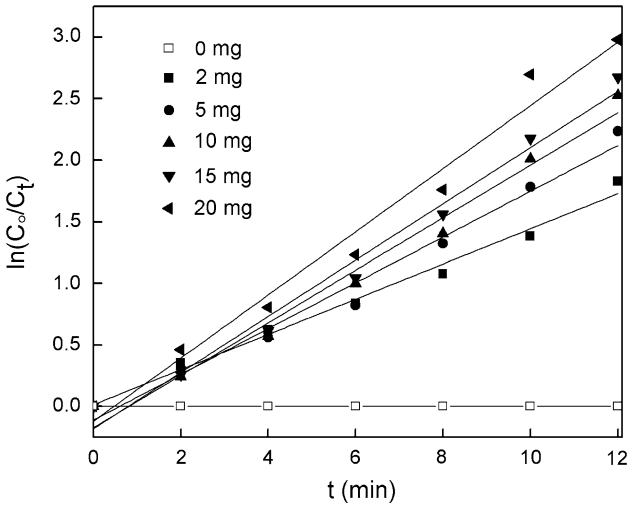

Figure 8 Plots of $\ln(C_0/C_t)$ versus the reaction time for the catalytic hydrogenation reduction of 4-NP in the presence of different amounts of CNT/CS/AgNP composites ([4-NP] = 37 mg/L, [$NaBH_4$] = 1.85 g/L).

immediately when the CNT/CS/AgNPs were added. The time-dependent absorption spectra showed a decrease in the intensity of the absorption peak at 400 nm and a concomitant increase of a new peak at 298 nm, indicating the generation of 4-aminophenol (4-AP). After about 20 min, the peak at 400 nm almost disappeared, indicating the completion of the catalytic reduction of the 4-NP.

The reaction rate was assumed to be independent of the concentration of sodium borohydride since this reagent was used in large excess. Therefore, the kinetic data could be fit with the first-order rate law [40]:

$$\ln(C_0/C_t) = kt.$$

Since the absorbance of 4-NP is proportional to its concentration, the ratio A_0/A_t (A_0 the initial absorbance; A_t the absorbance at time t of the solution) should be equal to the ratio of the corresponding concentrations of 4-NP (C_0/C_t). Indeed, a good linear relationship between $\ln(C_0/C_t)$ and reaction time was found for the catalytic reduction of 4-NP with different amounts of CNT/CS/AgNPs, as shown in Fig. 8. In Table 1, the value of rate constants (k) with different amounts of CNT/CS/AgNPs for the reduction of 4-nitrophenol in $NaBH_4$ solution was calculated from the slope of the straight line in Fig. 8. It was found that with the amount of CNT/CS/AgNPs increasing from 0, 2, 5, 10, 15, to 20 mg, the rate constant increased from 0 to 0.257 min^{-1}. Compared with other Ag catalysts as shown in Table 2, the rate constant of the prepared CNT/CS/AgNPs was higher than that of several polymer-, carbon-, and oxide-supported Ag composites, such as Ag nanoparticles supported poly[*N*-(3-trimethoxy silyl)propyl]aniline (Ag@PTMSPA) (0.22 min^{-1}) [41], poly(acrylamidoglycolic acid)/Ag

Table 1 The value of rate constant (k) with different amounts of CNT/CS/AgNPs for the reduction of 4-nitrophenol in $NaBH_4$ solution

CNT/CS/AgNPs (mg)	k (min^{-1})
2	0.162
5	0.186
10	0.206
15	0.226
20	0.257

Table 2 Comparison with different catalysts

Catalysts	k (min^{-1})	References
Ag@PTMSPA	0.22	[41]
Poly(acrylamidoglycolic acid)/Ag	0.0923	[42]
Carbon sphere/AgNPs	0.104	[43]
Ag/SiO_2NWs	0.15	[44]
Iron oxide/AgNPs	0.143	[45]
ESM fiber/AgNPs	0.25	[46]
Cellulose nanocrystals/AgNPs	0.255	[47]
CNT/CS/AgNPs	0.257	This work

composites (0.0923 min^{-1}) [42], carbon sphere/AgNPs (0.104 min^{-1}) [43], Ag/SiO_2NWs (0.15 min^{-1}) [44], and iron oxide/AgNPs (0.143 min^{-1}) [45]. Moreover, the catalytic rate of the CNT/CS/AgNPs was comparable to eggshell membrane (ESM) fiber/AgNP composites (0.25 min^{-1}) [46] and silver nanoparticles on cellulose nanocrystals (0.255 min^{-1}) [47]. According to these results, it was found that the AgNPs supported on the substrate with a hydrophilic surface had higher catalytic activities than those on the hydrophobic supports. This is because many hydrophilic supports possessed lots of hydroxyl, carbonyl, or amino groups, and these groups could grasp the reactants (borohydride ions and 4-NP molecules) more easily on the surface of AgNPs in the aqueous solution. Chitosan (CS) is a typical polymer containing many hydroxyl and amino groups. When a chitosan molecule was decorated on the surface of carbon nanotubes, the decorated CS helps generate CNT/CS/AgNPs, improving the ability of the catalytic reduction of 4-NP. However, the recyclability of CNT/CS/AgNPs has to be further improved. As shown in Fig. 9, CNT/CS/AgNPs were used for testing the catalytic reduction of 4-NP twice. It can be seen that the rate constant of the second test was 0.052 min^{-1}, which was much smaller than that of the first test (0.257 min^{-1}). The decreased catalytic ability may be due to the low recovery of CNT/CS/AgNPs dispersed in solution, e.g., the weight loss of the catalyst used at the first time can be up to 70 %. Further efforts are required in the future to recover the used CNT/CS/AgNP catalyst and to improve their recyclability.

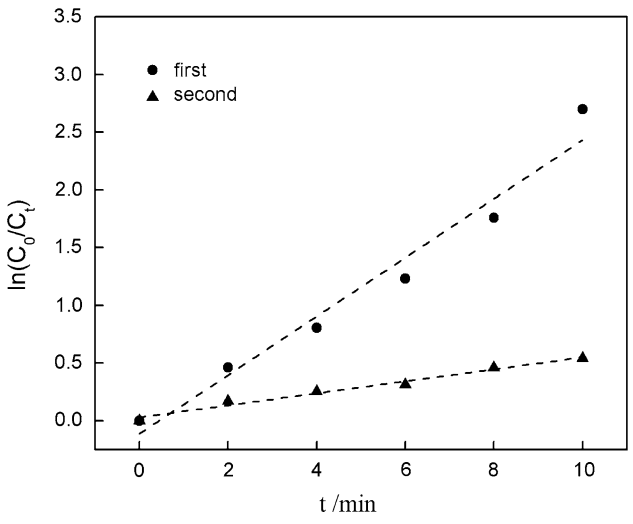

Figure 9 Plots of $\ln(C_0/C_t)$ versus the reaction time for the catalytic hydrogenation reduction of 4-NP with 20 mg CNT/CS/AgNP nanocomposites for reuse twice ([4-NP] = 37 mg/L, [$NaBH_4$] = 1.85 g/L).

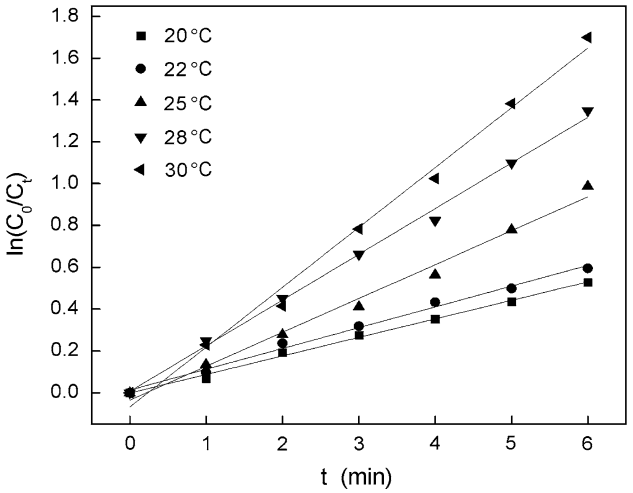

Figure 10 Plots of $\ln(C_0/C_t)$ versus the reaction time for the catalytic hydrogenation reduction of 4-NP with 4 mg CNT/CS/AgNP nanocomposites at different temperatures as indicated from 20 to 30 °C ([4-NP] = 37 mg/L, [$NaBH_4$] = 1.85 g/L).

In order to study the effect of reaction temperature on the catalytic activity of CNT/CS/AgNPs, the catalytic hydrogenation reduction of 4-NP with 4 mg CNT/CS/AgNP composites was conducted at temperature from 20 to 30 °C. As shown in Fig. 10, a good linear relationship between $\ln(C_0/C_t)$ and reaction time was obtained at different temperatures. The higher temperature corresponded to the larger value of rate constant and was favorable to enhance the rate constant of the catalytic hydrogenation reduction of 4-NP. Figure 11 shows a good

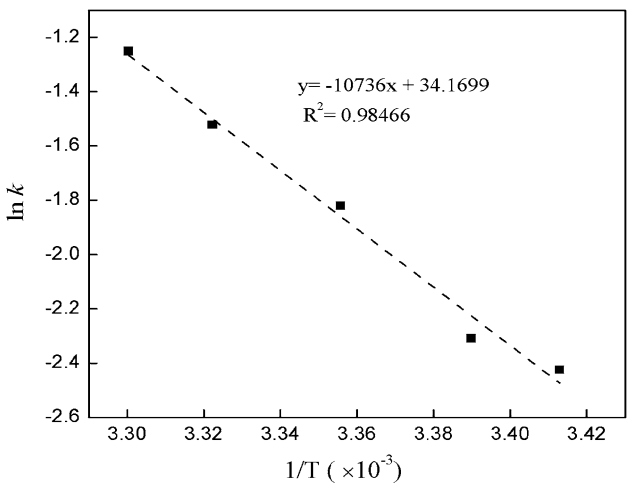

Figure 11 A plot for the relationship between ln k and $1/T$.

linear relationship between ln k and $1/T$, which accords with Arrhenius equation expressed as ln $k = \ln A - E_a/(RT)$, where A represents the Arrhenius factor; k is the rate constant of the reaction at temperature T (in Kelvin), and R is the universal gas constant. Therefore, the activation energy (E_a) was calculated to be 89.27 kJ mol^{-1} from the slope of the straight line, which was obviously lower than that of Ag nanoparticles on eggshell membrane (114.07 kJ mol^{-1}) [46]. This result demonstrates that the CNT/CS/AgNPs have good catalytic ability for the hydrogenation reduction of 4-NP.

Conclusions

In summary, a simple and environmentally friendly approach was demonstrated to prepare CNT/CS/AgNP composites. Chitosan, both serving as an effective reductant and an absorbent for the generation of AgNPs with an average size of 6 nm on the surface of CNTs, was loaded on the surface of carbon nanotubes. The weight ratio of silver in the CNT/CS/AgNP composites was found to be 18 %. The catalytic activity of CNT/CS/AgNP composites was evaluated by catalytic hydrogenation reduction of *p*-nitrophenol in sodium borohydride ($NaBH_4$) solution. The results showed that the as-prepared CNT/CS/AgNP composites had a high rate constant of 0.257 min^{-1} and an activation energy of 89.27 kJ mol^{-1}, exhibiting a highly catalytic activity.

Acknowledgements

This work was supported by the National Science Foundation of China (51203125), Discipline Innovation Team Project of Wuhan Textile University (201401020), and Technology Innovation Foundation of Wuhan Textile University (153002).

Conflict of interest The authors declare that they have no conflict of interest.

References

[1] Chung HT, Won JH, Zelenay P (2013) Active and stable carbon nanotube/nanoparticle composite electrocatalyst for oxygen reduction. Nat commun 4:1922

[2] Tammeveski L, Erikson H, Sarapuu A, Kozlova J, Ritslaid P, Sammelselg V, Tammeveski K (2012) Electrocatalytic oxygen reduction on silver nanoparticle/multi-walled carbon nanotube modified glassy carbon electrodes in alkaline solution. Electrochem Commun 20:15–18

[3] Liu CY, Hu JM (2009) Hydrogen peroxide biosensor based on the direct electrochemistry of myoglobin immobilized on silver nanoparticles doped carbon nanotubes film. Biosens Bioelectron 24(7):2149–2154

[4] Narang J, Chauhan N, Jain P, Pundir CS (2012) Silver nanoparticles/multiwalled carbon nanotube/polyaniline film for amperometric glutathione biosensor. Int J Biol Macromol 50(3):672–678

[5] Yuan W, Jiang G, Che J, Qi X, Xu R, Chang MW, Chan-Park MB (2008) Deposition of silver nanoparticles on multiwalled carbon nanotubes grafted with hyperbranched poly(amidoamine) and their antimicrobial effects. J Phys Chem C 112(48):18754–18759

[6] Mohan R, Shanmugharaj AM, Sung HR (2011) An efficient growth of silver and copper nanoparticles on multiwalled carbon nanotube with enhanced antimicrobial activity. J Biomed Mater Res B 96(1):119–126

[7] Ma PC, Tang BZ, Kim JK (2008) Effect of CNT decoration with silver nanoparticles on electrical conductivity of CNT-polymer composites. Carbon 46(11):1497–1505

[8] Fortunati E, D'angelo F, Martino S, Orlacchio A, Kenny JM, Armentano I (2011) Carbon nanotubes and silver nanoparticles for multifunctional conductive biopolymer composites. Carbon 49(7):2370–2379

[9] LeeáTan K (2001) Growth of Pd, Pt, Ag and Au nanoparticles on carbon nanotubes. J Mater Chem 11(9):2378–2381

[10] Liu Y, Tang J, Chen X, Chen W, Pang GKH, Xin JH (2006) A wet-chemical route for the decoration of CNTs with silver nanoparticles. Carbon 44(2):381–383

[11] Yang GW, Gao GY, Wang C, Xu CL, Li HL (2008) Controllable deposition of Ag nanoparticles on carbon nanotubes as a catalyst for hydrazine oxidation. Carbon 46(5):747–752

[12] Quinn BM, Dekke C, Lemay SG (2005) Electrodeposition of noble metal nanoparticles on carbon nanotubes. J Am Chem Soc 127(17):6146–6147

[13] Ma PC, Siddiqui NA, Marom G, Kim JK (2010) Dispersion and functionalization of carbon nanotubes for polymer-based nanocomposites: a review. Composites A 41(10):1345–1367

[14] Sun YP, Fu K, Lin Y, Huang W (2002) Functionalized carbon nanotubes: properties and applications. Acc Chem Res 35(12):1096–1104

[15] Balasubramanian K, Burghard M (2005) Chemically functionalized carbon nanotubes. Small 1(2):180–192

[16] Hou PX, Liu C, Cheng HM (2008) Purification of carbon nanotubes. Carbon 46(15):2003–2025

[17] Wildgoose GG, Banks CE, Compton RG (2006) Metal nanoparticles and related materials supported on carbon nanotubes: methods and applications. Small 2(2):182–193

[18] Avilés F, Cauich-Rodríguez JV, Moo-Tah L, May-Pat A, Vargas-Coronado R (2009) Evaluation of mild acid oxidation treatments for MWCNT functionalization. Carbon 47(13):2970–2975

[19] Likodimos V, Steriotis TA, Papageorgiou SK, Romanos GE, Marques RR, Rocha RP, Falaras P (2014) Controlled surface functionalization of multiwall carbon nanotubes by HNO_3 hydrothermal oxidation. Carbon 69:311–326

[20] Gao G, Pan M, Vecitis CD (2015) Effect of the oxidation approach on carbon nanotube surface functional groups and electrooxidative filtration performance. J Mater Chem A 3(14):7575–7582

[21] Liu Y, Tang J, Chen X, Xin JH (2005) Decoration of carbon nanotubes with chitosan. Carbon 43:3178–3180

[22] Murugadoss A, Chattopadhyay A (2008) A 'green' chitosan–silver nanoparticle composite as a heterogeneous as well as micro-heterogeneous catalyst. Nanotechnology 19:015603–015611

[23] Lin J, He C, Zhao Y, Zhang S (2009) One-step synthesis of silver nanoparticles/carbon nanotubes/chitosan film and its application in glucose biosensor. Sens Actuators B 137(2):768–773

[24] Hernández-Vargas J, González-Campos JB, Lara-Romero J, Prokhorov E, Luna-Bárcenas G, Aviña-Verduzco JA, González-Hernández JC (2014) Chitosan/MWCNTs-decorated with silver nanoparticle composites: dielectric and antibacterial characterization. J Appl Polym Sci 131(9):1–13

[25] Yeshchenko OA, Dmitruk IM, Alexeenko AA, Kotko AV, Verdal J, Pinchuk AO (2012) Size and temperature effects on the surface plasmon resonance in silver nanoparticles. Plasmonics 7(4):685–694

[26] Duval Malinsky M, Kelly KL, Schatz GC, Van Duyne RP (2001) Nanosphere lithography: effect of substrate on the localized surface plasmon resonance spectrum of silver nanoparticles. J Phys Chem B 105(12):2343–2350

[27] Twu YK, Chen YW, Shih CM (2008) Preparation of silver nanoparticles using chitosan suspensions. Powder Technol 185(3):251–257

[28] Wei D, Sun W, Qian W, Ye Y, Ma X (2009) The synthesis of chitosan-based silver nanoparticles and their antibacterial activity. Carbohydr Res 344(17):2375–2382

[29] Babu MG, Gunasekaran P (2009) Production and structural characterization of crystalline silver nanoparticles from Bacillus cereus isolate. Colloids Surf B 74(1):191–195

[30] Murugadoss A, Chattopadhyay A (2008) A 'green' chitosan–silver nanoparticle composite as a heterogeneous as well as micro-heterogeneous catalyst. Nanotechnology 19(1):015603

[31] Kweon H, Um IC, Park YH (2001) Structural and thermal characteristics of *Antheraea pernyi* silk fibroin/chitosan blend film. Polymer 42(15):6651–6656

[32] Carson L, Kelly-Brown C, Stewart M, Oki A, Regisford G, Luo Z, Bakhmutov VI (2009) Synthesis and characterization of chitosan–carbon nanotube composites. Mater Lett 63(6):617–620

[33] Bom D, Andrews R, Jacques D, Anthony J, Chen B, Meier MS, Selegue JP (2002) Thermogravimetric analysis of the oxidation of multiwalled carbon nanotubes: evidence for the role of defect sites in carbon nanotube chemistry. Nano Lett 2(6):615–619

[34] Vaidya MJ, Kulkarni SM, Chaudhari RV (2003) Synthesis of *p*-aminophenol by catalytic hydrogenation of *p*-nitrophenol. Org Process Res Dev 7(2):202–208

[35] Li J, Liu CY, Liu Y (2012) Au/graphene hydrogel: synthesis, characterization and its use for catalytic reduction of 4-nitrophenol. J Mater Chem 22(17):8426–8430

[36] Lu H, Yin H, Jiang T, Liu Y, Yu L (2008) Influence of support on catalytic activity of Ni catalysts in *p*-nitrophenol hydrogenation to *p*-aminophenol. Catal Commun 10(3):313–316

[37] Chiou JR, Lai BH, Hsu KC, Chen DH (2013) One-pot green synthesis of silver/iron oxide composite nanoparticles for 4-nitrophenol reduction. J Hazard Mater 248:394–400

[38] Hoseini SJ, Rashidi M, Bahrami M (2011) Platinum nanostructures at the liquid–liquid interface: catalytic reduction of *p*-nitrophenol to *p*-aminophenol. J Mater Chem 21(40):16170–16176

[39] Peng J, He R, Tan M, Dou Y, Wang Z, Chen GZ, Jin X (2015) Electrochemical preparation of fine powders of nickel-boron alloys in molten chlorides for magnetic hydrogenation catalysts. J Electrochem Soc 162(4):H271–H277

[40] Du Y, Chen H, Chen R, Xu N (2004) Synthesis of *p*-aminophenol from *p*-nitrophenol over nano-sized nickel catalysts. Appl Catal A 277(1):259–264

[41] Manesh KM, Gopalan AI, Lee KP, Komathi S (2010) Silver nanoparticles distributed into polyaniline bridged silica network: a functional nanocatalyst having synergistic influence for catalysis. Catal Commun 11(10):913–918

[42] Gao Y, Ding X, Zheng Z, Cheng X, Peng Y (2007) Template-free method to prepare polymer nanocapsules embedded with noble metal nanoparticles. Chem Commun 36:3720–3722

[43] Tang SC, Vongehr S, Meng XK (2010) Carbon spheres with controllable silver nanoparticle doping. J Phys Chem C 114:977–982

[44] Chiou JR, Lai BH, Hsu KC, Chen DH (2013) One-pot green synthesis of silver/iron oxide composite nanoparticles for 4-nitrophenol reduction. J Hazard Mater 248:394–400

[45] Zhang H, Duan T, Zhu W, Yao WT (2015) Natural chrysotile-based nanowires decorated with monodispersed Ag nanoparticles as a highly active and reusable hydrogenation catalyst. J Phys Chem C 119(37):21465–21472

[46] Liang M, Su R, Qi W, Yu Y, Wang L, He Z (2014) Synthesis of well-dispersed Ag nanoparticles on eggshell membrane for catalytic reduction of 4-nitrophenol. J Mater Sci 49(4):1639–1647. doi:10.1007/s10853-013-7847-y

[47] Tang J, Shi Z, Berry RM, Tam KC (2015) Mussel-inspired green metallization of silver nanoparticles on cellulose nanocrystals and their enhanced catalytic reduction of 4-nitrophenol in the presence of β-cyclodextrin. Ind Eng Chem Res 54(13):3299–3308